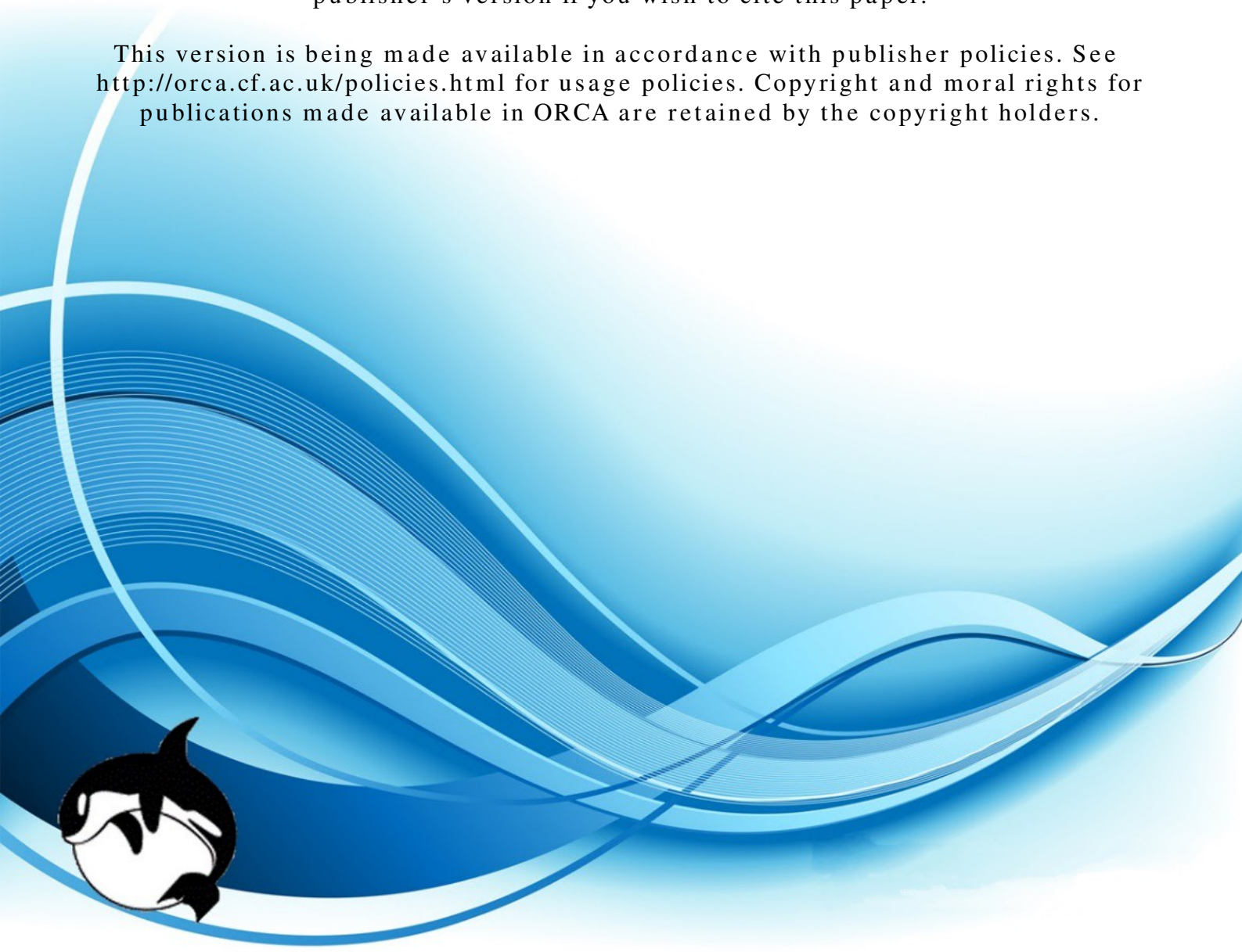

Synthesis of Engineering Surfaces using Representative Elementary Patterns of Roughness

Feodor M. Borodich[1] and Andrey Pepelyshev[2]

[1] College of Aerospace Engineering, Chongqing University, Chongqing, China,
[2] School of Mathematics, Cardiff University, Senghennydd Road, Cardiff CF24 4AG, UK

Abstract

Synthesis of surface roughness is a longstanding problem that has many practical applications. Here novel algorithms for synthesis of rough surfaces at nano/micro-scales are proposed. The algorithms are based on introduction and development of two new concepts, namely the representative elementary pattern of roughness (REPR) and the statistically representative pattern of surface roughness (SRPSR). From the statistical point of view, the REPR is the smallest interval (or area) over which a measurement can be made that represents statistically the whole surface. However, synthesis of surfaces by the direct use of the REPR may cause some artificial singularities. To avoid this drawback and to incorporate the synthetic surface in a numerical scheme of the contact solver, one needs to extend the REPR to a non-singular SRPSR that satisfies additional conditions of the scheme used. Our findings indicate that specific time series analysis techniques, such as the moving window approach, can be effectively utilized to extract the REPR from experimental data. The representativeness may be justified by the use of the Kolmogorov-Smirnov statistic. Extraction of REPRs of surfaces and constructions of appropriate SRPSRs are demonstrated on experimental data obtained by stylus and Atomic-Force Microscopy at micro and atomic/nano scales respectively.

1 Introduction

Measurements of the surface topography and analysis of roughness have been intensively studied for decades (see, e.g. Whitehouse 2010). Indeed, friction, wear and energy dissipation during interacting of engineering surfaces are strongly influenced by asperity deformations and these are controlled by the surface topography. Across various preparation methods, a defining characteristic of most engineering surfaces is the inherent presence of finite-scale roughness (see, e.g.

Khusu et al. 1975, Greenwood 1992, Grigoriev 2016). Surface roughness is a critical parameter influencing component performance across numerous industries, particularly in precision engineering applications. Surface roughness becomes particularly essential for understanding dry friction mechanisms in the absence of liquid lubricants, such as in nano/microscale devices and those operating in vacuum environments.

Nowadays there exist various solvers for numerical simulations of contact between rough solids, e.g. the Polonsky-Keer method (Polonsky and Keer 1999, 2000). Formally, one could use directly the real experimental roughness data in a contact solver. Advanced experimental techniques, exemplified by Atomic Force Microscopy (AFM), enable researchers to characterize surface topography with atomic-scale resolution (Bora et al. 2013). However, this would not allow the researchers to simulate many tribological phenomena. The difficulty may be described by the Lubrecht–Venner statement: though calculating a tribological problem for a single, real rough surface might be theoretically possible, its limited generalizability to other rough surfaces or even slight variations in the same surface renders it impractical (Lubrecht and Venner, 1999). Indeed, for such a prediction, one needs to have a warranty that the rough surface used in the contact solver is entirely typical of the whole surface on average at scales that are governing for the tribological process under consideration.

Surface synthesis statistically replicates the topographical characteristics of a real surface by creating a synthetic counterpart that mimics its statistical properties. Thus, synthesis of roughness is the crucial process for numerical and analytical simulations of contact between rough surfaces and other problems of tribology including friction and wear because the synthetic surfaces may be incorporated into numerical solvers of contact between rough surfaces.

Evaluation of statistical characteristics of surface roughness and synthesis of rough surfaces are longstanding research topics (see, e.g. Glover et al. 1998, Borodich and Bianchi 2013). Although synthesis of rough surfaces is widely used in various industries, the current statistical approaches to description of surface roughness are rather primitive. Indeed, despite the plethora of over 30 statistical roughness parameters in use, a clear understanding of how roughness influences dry contact and friction remains elusive (Nowicki 1985). Note that synthetic surfaces that model only some surface characteristics do not give a warranty that the rough surface used in the contact solver is entirely typical of the whole surface on average for the tribological process under consideration.

Consider a 2D/3D roughness profile with a large number of points, which is obtained by some technical device, e.g. by a profilometer or AFM. Let us study a problem of synthesis of another shorter 2D/3D profile that has the same height distribution as the large profile. Doing this, we may think that the large profile is obtained by a replication of some pattern given by the shorter profile. Two new concepts are introduced here: (i) the representative elementary pattern of roughness (REPR) and (ii) the statistically representative pattern of surface roughness (SRPSR). From the statistical point of view, the REPR is the smallest interval (or area) over which a measurement can be made that will yield a value representative of the whole surface, while the SRPSR not only ensures

statistical representativeness of the entire surface but also adheres to additional criteria based on the specific contact problem and numerical approach. It is proposed in the paper to modify some techniques of time series analysis (see, e.g. Golyandina and Zhigljavsky (2020)) and apply them to roughness of engineering surfaces. It is known that the Kolmogorov-Smirnov statistic may test whether the empirical distribution of data is different than a reference distribution. It is shown that the combination of the moving window technique and the Kolmogorov-Smirnov statistic effectively extracted the REPR of the surfaces. Hence, simpler surfaces with equivalent roughness in terms of the height distribution, may be synthesized. Contrary to the most current statistical approaches to surface roughness description, there is no need to assume the Gaussian distribution of heights or fractal character of roughness at the micro or atomic/nano scales.

2 Preliminaries. Synthesis of Tribological Surfaces.

2.1 The Fourier and wavelet approaches to synthesis of surfaces

Surface analysis often utilizes Fourier decomposition, breaking down the measurement data into a series of sine and cosine functions. In Fourier analysis of surfaces, the first harmonic reveals deviations of the measured profile from the nominal shape at a specific scale. If so, then this is attributed to surface waviness, while roughness may be considered as the noise of the surface shape. Thus, in surface topography, long wavelength features are termed "waviness", while short wavelength irregularities are classified as "roughness". It is often argued (Whitehouse 2010) that surface waviness should be measured apart from its roughness.

We will consider further only nominally flat surfaces. The intersection between a plane perpendicular to a surface and the surface itself is called the surface profile. The rough profile may be presented as graph of a function $z(x)$, $x \in [-L, L]$. Let $\bar{z}$ denote the mean profile line, i.e. $\bar{z} = \frac{1}{2L}\int_{-L}^{L} z(x)dx$ is the average value of the profile function $z(x)$. If the origin level of the height measurements is taken at $\bar{z}$ then

$$\frac{1}{2L}\int_{-L}^{L}[z(x) - \bar{z}]dx = 0.$$

The measurement data may be decomposed by the use of other orthogonal non-trigonometric functions. Usually such functions having compact supports are called wavelets and a decomposition of measurement data using such functions is called wavelet transform. Although there are several distinctions between the Fourier and wavelet approaches, the main idea of the wavelet transform is the same. One can use Fourier or wavelet synthesis, when the synthetic

surface is represented as the sum of the measurement decomposition using the bounded number of the basis functions (see, e.g. Greenwood 1992, Borodich and Bianchi 2013). Both kinds of surface synthesis do not provide a warranty that the surface obtained represents the original one and the Lubrecht–Venner statement (formulated in Section 1) is applicable to synthesized surfaces (Lubrecht and Venner, 1999).

2.2 Characterization of nominally flat surfaces.

Characterization of nominally flat surfaces may be roughly split into two partially overlapping approaches: (i) selection of several roughness parameters; and (ii) modelling of surface topography as a realization of a random process.

2.2.1 Surface description based on selected parameters of roughness.

Apparently, Abbott and Firestone (1933) pioneered the application of statistical tools to analyze surface roughness. They suggested to calculate the right-tailed cumulative distribution function of the surface heights $\Phi(z)$. If one considers the probability density function $\phi(z)$ that shows the probability that the height $z(x)$ at a surface point x is between z and $z + dz$, then $\Phi(z)$ is defined as

$$\Phi(z) = \int_z^\infty \phi(t)\, dt. \tag{1}$$

Tribology utilizes the Abbott-Firestone curve, also known as the bearing area curve, to potentially correlate it with the contact properties of rough surfaces. Its value at a level $z = h$ is equal to the normalized length (the area in the 2D problem) of the slice of the profile above the level h.

In some cases, this curve can be leveraged to estimate the force exerted during the penetration of a rough solid into an elastic foundation. Indeed, for a thin elastic layer contacting a punch with a large contact area compared to the layer's thickness, the leading term of the asymptotic solution can be approximated by the Fuss-Winkler foundation model (see, e.g. a review by Borodich et al. (2019a) and references therein).

Zhuravlev (1940) used the probability density function $\phi(z)$ and represented rough surfaces as collection of spherical protuberances having identical radii, but located at different heights. Then he developed his statistical model of contact between rough solids. A similar model was developed by Greenwood and Williamson (1966). Zhuravlev-Greenwood-Williamson type models require knowledge of the summit radii of surface asperities. If the roughness is isotropic then the surface roughness $z(x, y)$ is characterized by just a profile $z(x)$. If the profile heights $z_k = z(x_k)$ are measured with a regular stylus or AFM step τ, i.e. one has $x_k = x_0 + k\tau$, then the curvature (κ) of a protuberance z_k can be defined as

$$\kappa = -(z_{k-1} + z_{k+1} - 2z_k)/\tau^2$$

where $z_{k-1} < z_k$ and $z_{k+1} < z_k$, see (Greenwood 1992). Whitehouse and Archard (1970) demonstrated that the mean curvature of a rough surface is scale-dependent, varying with the chosen sampling interval.

The introduction of the Abbott-Firestone curve provoked a period of intense research, characterized by the generation of numerous statistical roughness parameters, called the "parameter rash" (Whitehouse 1982). The characterization encompassed both the vertical height distribution and the horizontal profile distribution of the roughness. Apparently the most popular height parameter is the maximum height R_{max} of the profile $z(x)$ defined on an interval $[-L, L]$ such that $\bar{z} = 0$, that is defined as

$$R_{max} = \max_{x \in [-L,L]} z(x).$$

The arithmetical mean deviation of the surface R_a, and the root mean square (rms) height R_q or σ^2 are also very popular parameters of surface roughness

$$R_a = \frac{1}{2L} \int_{-L}^{L} |z(x)|\, dx \approx \frac{\sum_{i=1}^{n} |z(x_i)|}{n}, \quad R_q = \sigma = \left[\frac{1}{2L} \int_{-L}^{L} [z(x)]^2\, dx \right]^{1/2}, \tag{2}$$

where n is the number of points of measurements on the interval and $z(x_i)$ is the measured height at the point x_i. Note that R_q is the square root of the mean square deviation with respect to the mean profile line $\bar{z} = 0$.

While certain statistical roughness parameters hold value in specific engineering applications, many lack general applicability (Whitehouse 1982). In fact, engineers have to describe the rough surfaces using just few roughness parameters. It is not clear what parameters they have to use for a particular tribological process under consideration because the European and British standard (BS-EN-ISO-4287:2000, (2009)) contains over 20 surface and profile parameters, while the American Standard (ASME B46.1-2002, 2002) is also a very long document, that includes all parameters of the European Standard and many additional parameters. In particular, it contains "Section 10 – Terminology and Procedures for Evaluation of Surface Textures Using Fractal Geometry". Despite claims of fractal dimension being a scale-independent roughness parameter, its fractal behavior typically holds only over a limited range of about 1.5 orders of magnitude (Borodich 2013). As it has been mentioned, there are many other parameters of surface roughness and it is practically impossible to include of them in synthetic surfaces. In general, the complex contact mechanics of rough surfaces defy description using a finite set of parameters.

2.2.2 Surface topography as a realization of a stochastic process.

Linnik and Khusu (1954, 1954a) suggested to model rough surfaces as realizations of Gaussian (normal) processes. Whitehouse and Archard (1970) introduced independently a similar approach and they noted correctly that a Gaussian surface is completely defined by two parameters, a height mean $\bar{z}$ and an

auto-covariance function $R(\delta)$

$$R(\delta) = \lim_{T\to\infty} \frac{1}{2T} \int_{-T}^{T} [z(x+\delta) - \bar{z}][z(x) - \bar{z}]\, dx = \langle [z(x+\delta) - \bar{z}][z(x) - \bar{z}] \rangle.$$

The function $R(\delta)$ characterizes the horizontal distribution of asperities of a rough surface profile. Indeed, Maugis (2000) emphasized the need to consider both vertical and horizontal roughness distributions, as surfaces can share height and peak height characteristics yet differ in horizontal extension. Instead of $R(\delta)$ one can use its Fourier transform, the power spectral density (PSD) $G(\omega)$ of the signal frequency ω

$$G(\omega) = \frac{2}{\pi} \int_0^{\infty} R(\delta) \cos\, \omega\delta\, d\delta \quad \text{and} \quad \bar{z} = \lim_{T\to\infty} \frac{1}{2T} \int_{-T}^{T} z(x)\, dx.$$

Gaussian surfaces were later intensively studied (see, e.g. Nayak (1971, 1973), Khusu et al. 1975, Greenwood 1992, Maugis 2000). Stochastic processes with non-Gaussian height distributions can be constructed using an approach described in (Bibby et al. 2005).

There exist various tests of normality of experimental data (Thode 2002). These include the Kolmogorov-Smirnov (KS), Lilliefors (LF), Shapiro-Wilk (SW), Anderson-Darling (AD), Cramer-von Mises (CVM), Pearson, and Shapiro-Francia (SF) normality tests. Applications of these tests to typical experimental data showed that (i) the height distribution is not normal either at nanometre or microscale for rough metallic surfaces prepared by grinding (Borodich et al. 2016); (ii) the height distribution is normal for polishing papers of different nominal asperity sizes (Pepelyshev et al. 2018); and (iii) AFM measurements at 117 nm steps revealed normality of microscale and nanoscale roughness for carbon coatings deposited by DC pulsed magnetron sputtering, while 10 nm steps identified a departure from normality in the roughness of the non-biased sample (Borodich et al. 2019b). Thus, the prevalence of non-Gaussian characteristics in real-world surfaces necessitates the exploration of alternative models beyond those designed for Gaussian landscapes.

2.2.3 Fractal and PSD approaches to surface roughness.

Many different surface topographies were studied by Sayles and Thomas (1978). They obtained an experimental relation between normalized PSD and wavelength. Logarithmic plotting yielded a remarkably consistent trend across a vast range, spanning micrometers to meters. Berry and Hannay (1978) argued that these results are a particular case of fractal surfaces. However, the PSD approach has not a lot of sense if it is applied to the measurement data without checking normality of the height distribution. Nevertheless the fractal approach was quite popular for characterization of rough surfaces and their synthesis.

There is a very popular claim that the surface topography shows self-affine fractal-like scaling, that is manifested as a power-law $G(\omega) \propto 1/\omega^{(1+2H)}$. Here H is the so-called Hurst exponent. The papers that develop the fractal approach

to surface topography are often claimed that the statistical properties of the topography are invariant under quasi-homogeneous transformation of coordinates (self-affinity in the fractal terminology), i.e. if $\mathbf{x} \to \lambda\mathbf{x}$, then $z(\mathbf{x}) \to \lambda^H z(\mathbf{x})$, where $z(\mathbf{x})$ is the surface topography height at point $\mathbf{x}$, λ is any positive scaling factor, and H is the so-called self-affine exponent or the Hurst parameter that describes the trend of the topography heights. The arguments that the Hurst parameter (exponent) that follows from the latter definition is the same as the above mentioned former one (it connects H with the power-law behaviour of the PSD) are rather vague.

Jetti and Ostoja-Starzewski (2022) wrote that the property of self-affinity relates to two key statistical parameters: the D (which represents the 'roughness') and H (which represents the 'spatial memory'). They repeated also the common statement about self-affine fractals that the exponent H is directly related to D and the Euclidean dimension E: $H = E - D$, where $E = 2$ for a profile and $E = 3$ for a surface.

The above claims and similar statements about universality of fractal nature of roughness caused development of various fractal approaches to surface roughness description. In fact (see, e.g. Borodich et al. 2020, 2024), a very rough surface and a polished surface can have the same D. Borodich (1998a,b) showed that for the parametric-homogeneous (PH) fractal functions (it is a special class of functions obeying the law of discrete self-similarity), the trend of a function (usually attributed to H) and its fractal dimension are not connected to each other. In fact, he showed that PH-functions may have arbitrary prescribed trends keeping the same D. Using the terminology by Jetti and Ostoja-Starzewski (2022), one can say that H and D are decoupled. The fractal approaches to surface topography are discussed in detail by Borodich et al. (2020). In particular, they argued that the both 'self-affine fractal' and 'Hurst exponent' terms are ill-defined.

Often the Weierstrass-Mandelbrot (W-M) fractal function is used as synthetic fractal surface for application in tribology. Majumdar and Bhushan (1990) suggested to use the following truncated W-M function

$$\tilde{W}(x;p) = \Lambda^{(D-1)} \sum_{n=n_1}^{\infty} p^{(D-2)n} \cos 2\pi p^n x, \quad 1 < D < 2, \quad p > 1, \qquad (3)$$

for representation of surface roughness. Here n_1 is an integer number, which corresponds to the low cut-off frequency of the profile, and Λ is the so-called characteristic length scale of the profile. The number n_1 depends on the length L of the sample and is given by $p^{n_1} = 1/L$ and the parameter Λ determines the position of the spectral density along the power axis. The graph of $\tilde{W}$ was suggested as a synthetic roughness profile with a power-law fractal behavior mimicking the fractal dimension of a real surface.

It was often argued that both parameters Λ and D of the function W or $\tilde{W}(x;p)$ are scale-invariant characteristics of the roughness. The W-M function was even considered as a general fractal distribution function for rough surface profiles (Blackmore and Zhou, 1996). However, the non-truncated Weierstrass-

Mandelbrot function is a particular case of parametric-homogeneous (PH) functions, and it is possible to construct a PH-function having prescribed fractal dimension and arbitrary trend (Borodich, 1998a,b). Hence, the W-M function cannot be considered as a general example of fractal roughness. Through illustrative examples, Borodich (1993, 1998a,b), and Borodich and Onishchenko (1993, 1999) demonstrated the insufficiency of fractal dimension alone in capturing the contact behavior of rough surfaces. In addition, Bhushan (1995) pointed out that experimental studies revealed non-uniqueness of the parameters Λ and D in the fractal model, highlighting their dependence on measurement instrumentation and resolution.

Although nowadays the fractal approach is less popular than it was about 20 years ago, the PSD approach is still actively used. However, the fractal and PSD approaches have the common drawback. If in addition to the profile $z(x)$ one considers an inverted profile $y(x)$ defined as $y(x) = -z(x)$, then the both profiles $z(x)$ and $y(x)$ have the same auto-correlation function and the power spectrum in both (x, z) and (x, y) coordinate systems. If $z(x)$ has a fractal graph, then, evidently, $y(x)$ has the same fractal dimension. Thus, neither fractal dimension nor PSD alone can give a full description of surface roughness.

3 Representative elementary pattern of roughness

Accurately representing rough surfaces typically necessitates the use of very large datasets capturing surface height information. This creates difficulties in application of conventional numerical methods, e.g. Polonsky-Keer method, to rough contact studies impractical. To achieve a requested numerical accuracy, the grid, on which fast Fourier transform (FFT) is performed, needs to be extended far beyond the contact area, leading to a substantial bottleneck in terms of computational time. However, the computations may be performed using smaller amount of measurement data, namely FFT can be applied on a smaller interval of the SRPSR or a close pattern. Let us introduce the notion of the representative elementary pattern of roughness mirroring the notion of the representative elementary volume used in mechanics of random inhomogeneous materials. As it has been mentioned, the REPR is the smallest interval (or area) over which a measurement can be made that will yield a value representative of the whole from the statistical point of view. It is impossible to possess a representative property for patterns smaller than the REPR.

3.1 The Kolmogorov-Smirnov statistic and moving window techniques

The Kolmogorov-Smirnov statistic (also known as the Kolmogorov-Smirnov Goodness of Fit test or the KS-test) compares the data of a sample and a given distribution or two samples and allows us to understand if they have the

same distribution (Conover 1999). If the Kolmogorov-Smirnov statistic is used to test if the distribution observed on a sample came from a specified theoretical distribution, e.g. the Gaussian distribution, then it is referred to as a one-sample KS-test. Examples of applications of the one-sample KS-test to check whether the surface roughness is normal, were given by Borodich et al. (2016) and Pepelyshev et al. (2018). If the Kolmogorov-Smirnov statistic is used to test whether two samples came from the same distribution, then it is referred to as a two-sample KS-test. The details of applications of the two-sample KS-test to subsamples extracted by moving windows are discussed in this section.

Consider a profile that is a sample of surface roughness measurements and another sample that is a subset of the whole profile. The hypotheses H_0 and H_1 of the KS-test are the following, H_0: the subset sample has the same population distribution as the whole profile; and H_1: the subset sample does not represent the full population distribution.

Moving window (or rolling window) techniques slide a selection window through the whole sample of measurements for analysis of the roughness data in the window. In such manner, moving window is used to select a subset sample. Because the total number of measurement points in the sample is fixed the moving window techniques are designed for retrospective application (Bower 2022, Golyandina and Zhigljavsky 2020, Schelter et al. 2006). Note that during movement of the window from left to right, a new point is added to the subset sample at the right and the left point is removed. In general, the moving window allows us to calculate various local statistical properties of the whole sample within the window. Due to the assumption that the profile is homogeneous and it contains a sufficient number of asperities for the apparent properties to be independent of the scale of consideration, it is expected that asperities for the REPR-based synthesized profile will be similar to asperities for the whole profile.

3.2 Extraction of the REPR

To resolve the problem formulated by Lubrecht and Venner (1999), we need to collect experimental measurements of the surface roughness (5-10 profiles) that may be considered as representative samples of the surface roughness. Let each of the samples have the same length N, that is, the total number of measurements on each profile is N. Applying the Kolmogorov-Smirnov statistic to each pair of these profiles, we can check if all these profiles have the same height distribution. If profiles are not similar to each other, this indicates that the surface is not homogeneous and should be studied by segments. If they are, then the procedure of extraction of the REPR for a surface can be formulated as follows. Create a joint profile by merging these several profiles. If we took m profiles then the length of the joint profile is equal to $K = mN$. To find the pattern, we slide a window of length N_s along each of m profiles and compute a similarity between the subset sample within the window and the joint profile using the Kolmogorov-Smirnov statistic. Then a REPR is constructed as a subset sample such that the statistical characteristics of the REPR are the same as the characteristics of the surface.

The algorithm of extraction of the REPR formally is as follows. First, we take the joint roughness profile if $m > 1$ or the single whole profile, which is a series of heights $z_1, z_2, \ldots, z_K$, where $K = mN$. Second, we take the length of the moving window as N_s, where $N_s < N$, and slide this window along each of the profiles. Specifically, for the starting point i, $0 \le i \le N - N_s$, we select the subset sample $(z_{j,i+1}; z_{i+2}; \ldots z_{j,i+N_s})$, which is a series of heights extracted by the sliding window from the j-th profile. Third, we compute a similarity between the long series $z_1, z_2, \ldots, z_K$ of the joint profile and the subset sample $(z_{j,i+1}; z_{i+2}; \ldots z_{j,i+N_s})$ within the moving window with the shift i using the Kolmogorov-Smirnov statistic

$$D_{K,N_s:j:i} = \sup_x \Big| F_{joint,K}(x) - F_{j,N_s}(x) \Big|,$$

where $F_{joint,K}(x)$ and $F_{j,N_s}(x)$ are the cumulative distribution functions for two samples, respectively. Fourth, for the fixed window length N_s, we define a subset sample which minimizes the Kolmogorov-Smirnov statistic with respect to the shift i. Also, we consider the KS-based distance measure defined by

$$D_K(N_s) = \min_{\substack{j=1,\ldots,m \\ i=1,\ldots,N-N_s}} D_{K,N_s:j:i} \tag{4}$$

as a function N_s. Finally, choose N_s such that the measure $D_K(N_s)$ is close to zero and N_s is not big.

The chosen value N_s is the length of the REPR and the corresponding subset sample which yields $D_K(N_s)$ is the REPR of the surface.

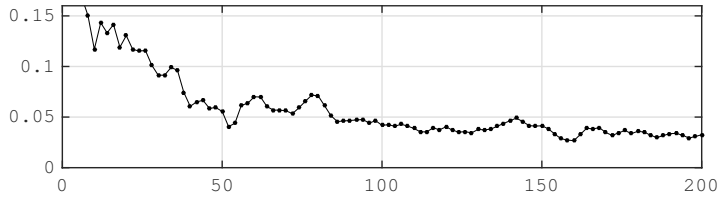

Figure 1: The KS-based distance measure $D_K(N_s)$ as a function of N_s for a roughness profile of a steel sample obtained by a profilometer, $K = N = 668$.

In Figure 1 we show a typical behaviour of the KS-based distance measure $D_K(N_s)$. We can see that $D_K(N_s)$ has the decreasing tendency on N_s. For very small N_s, the measure $D_K(N_s)$ is large because a very short segment cannot sufficiently well represent the whole profile. In addition, we have $D_K(N_s) \approx 0$ for large N_s because the large segment is similar to the whole profile. We recommend to choose N_s as the smallest integer such that $D_K(N_s) < 0.05$. For example, in Figure 1 candidates for N_s would be just over 50 or around 80. If N_s also satisfies the constraint $N_s = 2^b$ for some integer b, then the REPR with 2^b points will be called the FFT-REPR.

4 Construction of the SRPSR

Formally, one could use the REPR obtained in a numerical solver for simulation of contact between rough surfaces. However, as one can see in the following figures, usually the height for the last point is not equal to the height for the first point of the REPR. Consequently, the formal employment of the REPR will cause artificial jumps in the synthetic profile and, in turn, the singularities of the stress fields. Hence, the SRPSR must not only be statistically representative of the entire surface but also adhere to additional criteria specific to the chosen contact problem formulation and numerical approach.

Note that any pattern that includes the REPR is also a representative pattern of surface roughness. If the numerical solver does not have any restriction on the number of the points in the SRPSR, then a pattern of the length $2N_s$ obtained from the REPR by its mirror symmetry can be taken as the SRPSR. Indeed, the heights at the first point and at the last point are the same and, therefore, there are no artificial singularities in the profile.

In fact, the solvers can have restrictions on the number of the points in the profile. Let consider as an example the Polonsky-Keer numerical scheme. The Polonsky-Keer algorithm combines the use of the FFT and the multi-level multi-summation techniques. This allows to reduce greatly the number of arithmetic operations required by the algorithm (Polonsky and Keer 2000). However, the employment of FFT requires that the profile contains 2^b points where b is some integer. Hence, we will need to extend the length of the pattern and include several additional points that the total length of the pattern will satisfy this condition. For example, if $N_s = 52$, then we need to add 12 additional points to extend the profile to a FFT-REPR having 2^6 points and then to use the mirror symmetry of the pattern. Hence, the final length of the SRPSR is 2^7.

4.1 Metallic surfaces

Tribological characterization of grinding-induced roughness on engineering surfaces has been performed across nano and micro scales to understand surface features. The heights of the micro-asperities were determined by the stylus profilometer (Taylor Hobson Form Talysurf 2 profilometer), while the data for nano/atomic scale was obtained by the AFM instrument (XE-100 from Park Systems). The resolution scales of the AFM device is 2 nm vertically and 5 nm laterally. The profilometer is fitted with a 250 nm in the x (measurement) direction, 1 micron in the y direction and 19 nm vertically. Let us study several datasets obtained by these instruments.

In Figure 2, one can see a roughness profile of a bronze sample obtained by AFM, where measurements z_k are taken at points $x_k = 0.1758k\,\mu m$, $k = 1, \ldots, K$, $K = 256$. The REPR of length 104 was extracted. Then it have been extended to the FFT-REPR having 128-points.

In Figure 3 we show the roughness profile of a copper sample obtained by AFM, where measurements z_k are taken at points $x_k = 0.15625k\,\mu m$, $k = 1, \ldots, K$, $K = 256$, the REPR of length 55 that have been extended to the

FFT-REPR having 64 points.

Figure 4 presents the roughness profile obtained by profilometre on a steel gear surface, where measurements z_k are taken at points $x_k = 1.5k\,\mu m$, $k = 0, 1, 2, \ldots, K$, $K = 667$; the REPR of length 53 that have been extended to the FFT-REPR having 64 points.

Comparing profiles in Figures 2–4 we see that the REPR for the bronze sample is longer than the REPR for the copper sample and a steel gear surface because shorts segments of the bronze roughness profile are very different from each other.

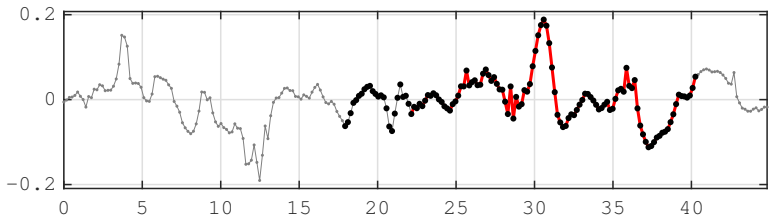

Figure 2: The REPR (red color) of length 104 and the FFT-REPR having 128 points (black dots) for a roughness profile of the bronze sample measured by AFM, scale units are μm.

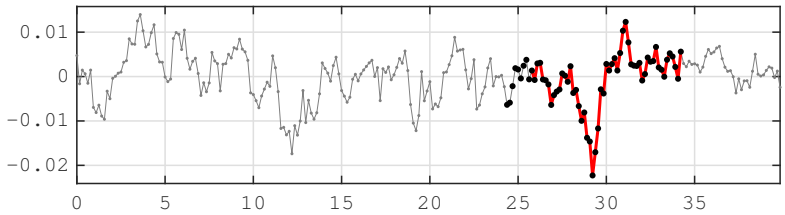

Figure 3: The REPR (red color) of length 55 and the FFT-REPR having 64 points (black dots) for a roughness profile of the copper sample measured by AFM, scale units are μm.

4.2 Carbon coating and PDMS

We consider the roughness of two amorphous carbon (a-C) films which were deposited on silicon substrates by DC-pulsed magnetron sputtering in Ar atmosphere (5×10^{-3} mbar) using a graphite target at 300 W. The pulse conditions were set at 250 kHz of frequency, 496 ns of duration (87.6% of duty cycle). A negative bias of approximately 150 V was applied to the substrate in one of the cases. Both processes were carried out at room temperature and the measured

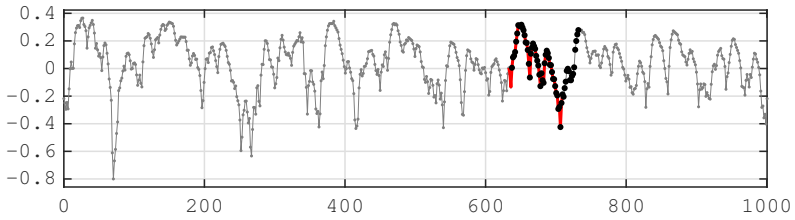

Figure 4: The REPR (red color) of length 53 and the FFT-REPR having 64 points (black dots) for a roughness profile of the steel sample measured by profilometer, scale units are μm.

thicknesses were 700 and 1300 nm for biased and non-biased samples, respectively. Carbon-based coatings prepared by plasma-assisted deposition methods at room temperature are generally amorphous as they are synthetized in conditions out of thermodynamic equilibrium. There are many papers based on DLC and a-C coatings where these structural characteristics are proven (see, e.g. Lin et al., 2010).

Hardness measurements carried out with a MTS Nanoindenter II XP using the continuous stiffness measurement (CSM) technique and a diamond Berkovich (three-sided pyramid) indenter tip gave 43 (biased) and 14 (non-biased) GPa, respectively. Scanning electron microscopy (SEM) data were recorded in a FEG Hitachi S4800 microscope operating at 5 kV.

The AFM system used to measure the nanoscale topography of the sample was the XE-100 model from Park Systems. The probes employed were the CSG model from NT-NDT. These probes are utilised for contact mode AFM operations and are designed with a rectangular-type cantilever, which is Au-coated on its reflective side. These probes are made of single crystal silicon and have a nominal force constant of 0.11 N/m, as stated by the manufacturer. The typical curvature radius of the tip mounted at the free of the cantilever is stated to be 6 nm. In particular, the dimension of a scanned area was set at 30 μm x 30 μm for the a-C sample. However, the scanned area was 40 μm x 40 μm for the bias a-C sample. In all cases 256 x 256 grid was used. This means that the AFM step was 117 nm for the area 30 μm x 30 μm and 156 nm nm for the area 40 μm x 40 μm respectively.

In Figure 5 we show a roughness profile of the a-C sample, the REPR of length 53 and the FFT-REPR having 64 points.

In Figure 6 we show a roughness profile of the a-C (bias) sample, the REPR of length 48 and the FFT-REPR having 64 points.

Finally, we consider the roughness of polydimethylsiloxane (PDMS) polymer. This material was used earlier by Purtov et al. (2013) to prepare epoxy resin replicas of surfaces having different topography and conduct depth-sensing indentation of the samples using a micro-force tester with a spherical smooth probe made of the compliant polydimethylsiloxane polymer in order to compare

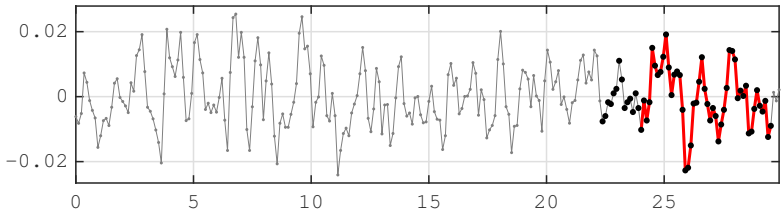

Figure 5: The REPR (red color) of length 53 and the FFT-REPR having 64 points (black dots) for a roughness profile of the a-C sample measured by AFM, scale units are μm.

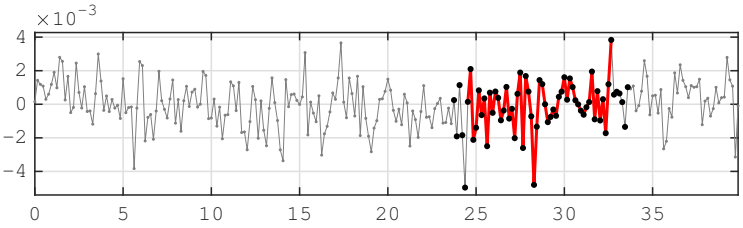

Figure 6: The REPR (red color) of length 48 and the FFT-REPR having 64 points (black dots) for a roughness profile of the a-C (bias) sample measured by AFM, scale units are μm.

values of the force of adhesion to the surfaces. In particular, a clean smooth glass surface and polishing papers of nominal asperity size 0.3 μm were used as templates for preparation of the epoxy resin replicas. The roughness of test surfaces was measured using a white light interferometer (Zygo NewView 6000; Zygo Corporation, Middlefield, CT, USA) at a magnification of 50. As it has been mentioned above, the roughness of the samples were tested by Pepelyshev et al. (2018).

In Figure 7 we show the roughness profile of the PDMS polymer, the REPR of length 84 and and the FFT-REPR having 128 points.

As it can be seen, the SRPSRs obtained for all samples are shorter than the original profiles. If the algorithms for solving the contact problems between rough surfaces do not require their extensions to 2^b points, then the appropriate SRPSRs may be extended in other ways.

5 Conclusion

It is known that the vast amount of data required for realistic descriptions of rough surfaces renders conventional numerical methods in contact mechanics computationally prohibitive. There were developed various effective numerical

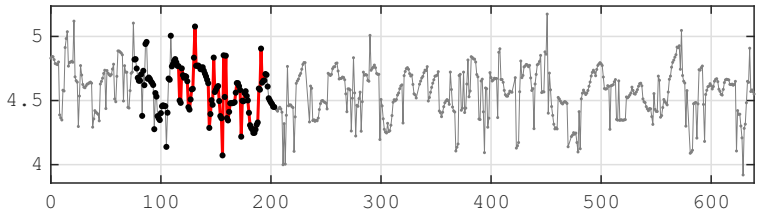

Figure 7: The REPR (red color) of length 84 and the FFT-REPR having 128 points (black dots) for a roughness profile of the PDMS polymer sample with nominal roughness 0.3 measured by white light interferometry, scale units are μm.

solvers for simulations of contact between rough surfaces, e.g. the Polonsky-Keer solver based on employement of FFT (Polonsky and Keer 2000). However, to achieve a requested numerical accuracy, the grid, on which FFT is performed, needs to be extended far beyond the contact area, leading to an essential growth of the computation time. It has been presented a fundamentally new approach to problems related to synthesis of rough surfaces of solids. The approach is based on introduction of a new concept, the representative elementary pattern of roughness that is the smallest interval (or area) over which a measurement can be made that represents statistically the whole surface. The idea of the REPR term is similar to the idea of the representative elementary volume used in mechanics of random inhomogeneous materials (Willis 1981).

It has been shown that statistical time series analysis methods, such as the moving window technique, have proven effective in extracting the REPR from experimental data. The two-sample Kolmogorov-Smirnov test (the KS statistic) have been used to compare the distribution of the sample within the moving window and the distribution of the whole sample. Hence, statistically, the REPR replicates the original rough surface, capturing its essential characteristics for analysis.

Usually, the synthesized surface cannot be viewed as a union of several copies of the REPR. Indeed, a series of REPRs will produce jumps at the joints of two REPRs, that in turn, cause singularities in stress fields of contacting solids. Hence, there is a need to find such size of moving window and its location that the appropriate pattern satisfies not only the condition that it is entirely typical of the whole surface but also satisfies some additional conditions depending on the contact problem formulation and the numerical scheme used. This reason caused the need in introduction of another new concept which is the statistically representative pattern of surface roughness (SRPSR).

Extraction of REPRs of surfaces and constructions of appropriate SRPSRs are demonstrated on experimental data obtained at micro and atomic/nano scales for several metallic surfaces, amorphous carbon and polymer samples. We argue that surfaces synthesized using our approach cannot be distinguished

from the original rough surface and they are convenient for the use of numerical algorithms based on employment of FFT techniques.

References

[1] Abbott, E.J. and Firestone, F.A. (1933) Specifying surface quality: a method based on accurate measurement and comparison. *Mechanical Engineering*, **55**, 569–572.

[2] ASME B46.1-2002 (2002) Surface Texture (Surface Roughness, Waviness and Lay). An American National Standard. ASME.

[3] Berry, M.V. and Hannay, J.H. (1978) Topography of random surfaces. *Nature*, **273**, 573.

[4] Bibby, B.M., Skovgaard, I.M. and Sorensen, M. (2005) Diffusion-type models with given marginal distribution and autocorrelation function. *Bernoulli*, 11(2), 191–220.

[5] Bhushan, B. (1995) A fractal theory of the temperature distribution at elastic contacts of fast sliding surfaces. - Discussion. *Trans. ASME. J. Tribology*, **117**, 214–215.

[6] Blackmore, D., and Zhou, J. G. (1996). A general fractal distribution function for rough surface profiles. *SIAM Journal on Applied Mathematics*, 56(6), 1694–1719.

[7] Bora, C.K., Plesha, M.E., and Carpick, R.W. (2013) A numerical contact model based on real surface topography. *Tribol. Lett.*, 50, 331–347.

[8] Borodich, F.M. (1993) Similarity properties of discrete contact between a fractal punch and an elastic medium. *C. r. Ac. Sc. (Paris), Ser. 2*, **316**, 281–286.

[9] Borodich, F.M. (1998a) Parametric homogeneity and non-classical self-similarity. I. Mathematical background. *Acta Mechanica*, **131**, 27–45.

[10] Borodich, F.M. (1998b) Parametric homogeneity and non-classical self-similarity. II. Some applications. *Acta Mechanica*, **131**, 47–67.

[11] Borodich F.M. (2013) Fractal Contact Mechanics. In: *Encyclopedia of Tribology: Wang, Q.J.; Chung, Y-W, (Eds.)*, Springer, **2**, 1249–1258

[12] Borodich F.M. and Bianchi D. (2013) Surface Synthesis Based on Surface Statistics, In: *Encyclopedia of Tribology: Wang, Q.J.; Chung, Y-W, (Eds.)*, Springer, **2**, 3472–3478.

[13] Borodich F.M., Galanov B.A., Perepelkin N.V., Prikazchikov D.A. (2019a) Adhesive contact problems for a thin elastic layer: Asymptotic analysis and the JKR theory. *Mathematics and Mechanics of Solids*, **24**(5), 1405–1424.

[14] Borodich, F.M., Brousseau, E., Clarke, A., Pepelyshev, A., Sanchez-Lopez, J.C. (2019b) Roughness of deposited carbon-based coatings and its statistical characteristics at nano and microscales. *Frontiers in Mechanical Engineering*, **5**, 73–82.

[15] Borodich, F.M., Jin, X., Pepelyshev, A. (2020) Probabilistic, fractal, and related techniques for analysis of engineering surfaces. *Frontiers in Mechanical Engineering*, **6**, article number: 64.

[16] Borodich, F.M. and Onishchenko, D.A. (1993) Fractal roughness for problem of contact and friction (the simplest models). *J. Friction Wear*, **14**, 452–459.

[17] Borodich, F.M. and Onishchenko, D.A. (1999) Similarity and fractality in the modelling of roughness by a multilevel profile with hierarchical structure. *Int. J. Solids Struct.*, **36**, 2585–2612.

[18] Borodich F.M., Pepelyshev A., Savencu O. (2016) Statistical approaches to description of rough engineering surfaces at nano and microscales. Tribol. Int. 103, 197–207.

[19] Borodich F.M., Pepelyshev A., Jin X. (2024) A Multiscale Statistical Analysis of Rough Surfaces and Applications to Tribology. *Mathematics*, **12**, 1–19.

[20] Bower, T. (2022) Introduction to Computational Engineering with MATLAB. Chapman and Hall/CRC. Abingdon, Oxon.

[21] BS-EN-ISO-4287:2000 (2009) Geometrical product specification (GPS) - Surface texture: Profile method - Terms, definitions and surface texture parameters. EN ISO 4287:1998+A1:2009.

[22] Conover W.J. (1999) Practical Nonparametric Statistics. New York, John Wiley and Sons.

[23] Glover, P.W.J., Matsuki, K., Hikima, R. and Hayashi, K. (1998) Synthetic rough fractures in rocks. *J. Geophysical Research-Solid Earth*, **103**, No.B5, 9609-9620.

[24] Golyandina, N., Zhigljavsky, A. (2020) Singular Spectrum Analysis for Time Series. Springer, Berlin, Heidelberg.

[25] Greenwood, J.A. (1992) Problems with surface roughness. In: Fundamentals of Friction, (Eds. I.L. Singer and H.M. Pollock). Kluwer, Boston, 57–76.

[26] Greenwood, J.A. and Williamson, J.B.P. (1966) Contact of nominally flat surfaces. *Proc. R. Soc. Lond.*, **A 370**, 300–319.

[27] Grigoriev A.Ya. (2016) Physics and Microgeometry of Technical Surfaces. Minsk, Belaruskaya Navuka (Russian)

[28] Jetti Y.S. and Ostoja-Starzewski M. (2022) Elastic contact of random surfaces with fractal and Hurst effects. doi.org/10.1098/rspa.2022.0384

[29] Khusu, A.P., Vitenberg, Yu.R., and Palmov, V.A. (1975) *Roughness of Surfaces: Theoretical Probabilistic Approach*. Nauka, Moscow (in Russian).

[30] Lin J., Moore J.J., Sproul, W.D., Mishra B,, Wu Z., Wang J. (2010) The structure and properties of chromium nitride coatings deposited using dc, pulsed dc and modulated pulse power magnetron sputtering, *Surf. Coat. Technol.*, 204, 2230-2239.

[31] Linnik, Yu.V. and Khusu, A.P. (1954a) Mathematical and statistical description of unevenness of surface profile at grinding. *Uspekhi Matematicheskikh Nauk*, **9**(3), 255 (Russian).

[32] Linnik, Yu.V. and Khusu, A.P. (1954) Mathematical and statistical description of unevenness of surface profile at grinding. *Bul. USSR Acad. Sci. Div. Techn. Sci.*, No. 20, 154–159. (in Russian).

[33] Lubrecht, A.A. and Venner, C.H. Elastohydrodynamic lubrication of rough surfaces. *Proc. Instn. Mech. Engrs. Part J. J. Eng. Trib.*, **213**, (1999) 397–404.

[34] Maugis, D. (2000) Contact, Adhesion and Rupture of Elastic Solids. Springer-Verlag, Berlin.

[35] Majumdar, A. and Bhushan, B. (1990) Role of fractal geometry in roughness characterization and contact mechanics of surfaces. *Trans. ASME. J. Tribology*, **112**, 205–216.

[36] Nayak, P.R. (1971) Random process model of rough surfaces. *ASME J. Lub. Tech.*, **93**, 398–407.

[37] Nayak, P.R. (1973) Some aspects of surface roughness measurement. *Wear*, **26**, 165–174.

[38] Nowicki, B. (1985) Multiparameter representation of surface roughness. *Wear*, **102**, 161–176.

[39] Pepelyshev, A., Borodich, F.M., Galanov, B.A., Gorb, E.V., Gorb, S.N. (2018) Adhesion of Soft Materials to Rough Surfaces: Experimental Studies, Statistical Analysis and Modelling. *Coatings*, 8(10), 350.

[40] Polonsky, I.A., Keer, L.M. (1999) A numerical method for solving rough contact problems based on the multi-level multi-summation and conjugate gradient techniques. *Wear*, 231, 206-219.

[41] Polonsky, I.A., Keer, L.M. (2000) Fast methods for solving rough contact problems: a comparative study. *Journal of Tribology*, 122, 36-41.

[42] Purtov, J., Gorb, E.V., Steinhart, M., Gorb, S.N. (2013) Measuring of the hardly measurable: adhesion properties of anti-adhesive surfaces. *Appl. Phys.*, 111, 183-189.

[43] Sayles, R.S. and Thomas, T.R. (1978) Surface topography as a nonstationary random process. *Nature*, **271**, 431–434.

[44] Schelter B., Winterhalder M., Timmer J. (2006) Handbook of time series analysis., Wiley-VCH. Weinheim.

[45] Thode, H.C. (2002) Testing for Normality. Marcel Dekker: New York.

[46] Whitehouse, D.J. (2010) Handbook of Surface and Nanometrology. Boca Raton, CRC Press.

[47] Whitehouse, D.J. (1982) The parameter rash - is there a cure? *Wear*, **83**, 75-78.

[48] Willis, J.R. (1981) Variational and related methods for the overall properties of composites. *WAdvances in Applied Mechanics*, **21**, 1-78.

[49] Whitehouse, D.J. and Archard, J.F. (1970) The properties of random surfaces of significance in their contact. *Proc. R. Soc. Lond.*, **A 316**, 97–121.

[50] Zhuravlev, V.A. (1940) On question of theoretical justification of the Amontons-Coulomb law for friction of unlubricated surfaces. Engl. Transl. (2007) *Proc. Instn. Mech. Engrs. Part J. J. Eng. Trib.*, **221**, 397–404.